Synthetic Metals 159 (2009) 1319–1324

Contents lists available at ScienceDirect

Synthetic Metals

journal homepage: www.elsevier.com/locate/synmet

Mesomorphism of dialkylterthiophene homologues

Nicolas Boucher[a], Julie Leroy[b], Sergey Sergeyev[b], Eric Pouzet[b], Vincent Lemaur[c], Roberto Lazzaroni[c], Jérôme Cornil[c], Yves Henri Geerts[b], Michele Sferrazza[a,*]

[a] Département de Physique, Faculté des Sciences, Université Libre de Bruxelles, Boulevard du Triomphe, CP223, 1050 Bruxelles, Belgium
[b] Laboratoire de Chimie des Polymères, Université Libre de Bruxelles, Boulevard du Triomphe, CP206/01, 1050 Bruxelles, Belgium
[c] Service de Chimie des Matériaux Nouveaux, Université de Mons-Hainaut/Materia Nova, Mons, Belgium

ARTICLE INFO

Article history:
Received 7 November 2008
Received in revised form 24 February 2009
Accepted 28 February 2009
Available online 9 April 2009

Keywords:
Dialkyterthiophenes
Organic semiconductors
Liquid crystals
Transition temperatures
Smectic mesophases

ABSTRACT

New dialkylterthiophene liquid crystalline compounds were synthesised and characterised using differential scanning calorimetry (DSC), X-ray diffraction (XRD) and polarized optical microscopy (POM). Upon cooling from the isotropic state to the crystalline phase, these dialkylterthiophenes present different types of smectic mesophases. For the highest ordered smectic phase, XRD analyses have revealed a molecular organisation within the smectic layers and the key structural parameters are determined by molecular modelling simulations. The structural properties of these smectic phases are discussed in relation to the alkyl chain length.

1. Introduction

Oligothiophenes have been attracting increasing attention in recent years due to their high charge carrier mobility, which could potentially be used in electronic devices, such as organic field-effect transistors (OFETs) [1,2]. However, the practical application of polycrystalline materials for OFET devices is often hampered by structural defects and grain-boundary effects, which dramatically decrease the charge carrier mobility [3]. Conjugated compounds possessing liquid crystalline phases are recognised as organic semiconductors of particular interest, having the properties of self-healing of structural defects and of self-organization in large structurally homogeneous domains [4]. A previous study of sexithienyl has in fact showed that large domains, only observed in the first two molecular layers, dominate the charge transport [5]. The importance of organisation in the first molecular layers was also shown to be crucial for semiconducting conjugated polymers: this was relevant to achieve high charge mobility via two-dimensional transport in self-organized conjugated lamellae [6].

In recent years, the synthesis of conjugated compounds and characterisation of liquid crystal phases, both of calamitic and discotic type, have been the subject of intense work, with the goal of developing liquid crystal phases in the form of thin films made up of monodomains uniformly aligned on the substrate. Moreover the control of the transition temperature to the liquid crystal phase for thin films and the manufacture of organic field-effect transistors are also crucial steps in order to optimise the properties of the electroactive molecular structures [7,8]. Finally, since the charge transport occurs within a few monolayers from the gate dielectric, it is also necessary to optimise the surface structure of the dielectric layer used in the field-effect transistor [9,10].

The symmetrical α,α′-disubstituted oligothiophenes have shown an enhanced chemical and electrochemical stability compared to Pentacene, Phthalocyanines and other small molecules [11]. In addition, a combination of a rigid aromatic core and flexible side chains in the structure of the α,α′-dialkyloligothiophenes induces the formation of liquid crystalline mesophases [12]. Dialkylterthiophenes exhibit complex phase behaviour where several thermotropic smectic phases are often observed [13].

A large body of work has been carried out to characterise these compounds, in particular in terms of the charge transport mobility, which demonstrated the influence of the molecular packing on the electrical performances. Nevertheless a fundamental understanding of the subtle relationship between the molecular structure of the organic semiconductors and their phase-forming behaviour is an important step for their potential use in organic electronics [14]. Such an understanding of molecular organisation is also necessary in order to comprehend the implications in the processing/manufacturing phases [15]. This calls for joint experimental and modelling approaches in which the molecular structure is systematically varied and correlated to the mesophases.

* Corresponding author. Tel.: +32 2 6505758.
E-mail address: msferraz@ulb.ac.be (M. Sferrazza).

0379-6779/$ – see front matter © 2009 Elsevier B.V. All rights reserved.
doi:10.1016/j.synthmet.2009.02.041

We have synthesised here a series of symmetrical α,α′-dialkyloligothiophenes and characterised their liquid crystal phases. We report a detailed study on a series of dialkylterthiophenes using various experimental techniques – X-ray diffraction (XRD), differential scanning calorimetry (DSC) and polarized optical microscopy (POM) – which are complemented by theoretical simulations of the molecular packing.

2. Experimental

Very recently, we reported on a practical and high-yield one-step synthesis of α,α′-di(*n*-alkyl)oligothiophenes followed by alkylation with *n*-alkylhalides [16]. The use of *t*BuOK to enhance the reactivity of dilithiated oligothiophene species towards alkylating agents was demonstrated to be of crucial importance. The full synthesis procedure is reported in Refs. [16,17]. Fig. 1 shows the chemical formula of dialkylterthiophenes. Alkyl chains of increasing length $-C_nH_{2n+1}$, with $n = 5–10$, have been used.

The physical characterisation of the compounds was performed using DSC, XRD and POM. A Mettler Toledo DSC 821 was used. A typical amount of 5 mg was scanned under nitrogen atmosphere at a rate of 5 °C min^{-1} between −10 and 150 °C.

XRD experiments for the characterisation of the different phases were carried out with a Bruker D8-diffractometer using the Cu Kα ray (λ = 1.5418 Å) in Bragg–Brentano geometry (θ–θ). The powder was placed on a 1-mm thick aluminium substrate placed on a heating stage operated at a cooling rate of 1 °C min^{-1} with an accuracy of 0.1 °C on the temperature. The X-ray measurements have been performed for each mesophase observed, as determined by DSC. POM analysis was performed with a Nikon Eclipse 80i polarizing microscope in order to observe the optical textures. Sample temperatures were controlled using a Mettler FP82 hot stage at a cooling rate of 1 °C min^{-1}. The compounds were placed between two glass plates and the images were recorded during the cooling of the sample.

3. Theoretical methodology

In order to simulate X-ray diffractograms, we first built unit cells containing two molecules, which were then replicated using periodic boundary conditions to produce infinite systems. Since the typical arrangement in a smectic phase is a tilted packing [18], the two molecules have been put parallel to each other in the unit cell and point in opposite directions, as a preliminary analysis of the experimental diffractograms has revealed the presence of two inequivalent molecules. Another evidence of this anti-parallel arrangement is that in this way the dipole moments of the isolated molecules cancel each other within the unit cell so that the crystal has not a net dipole moment. The unit cells have then been optimized at the molecular mechanics level with the COMPASS force field [19], using the default parameters implemented in the Materials Studio 4.0 package [20]. Ewald summation [21] has been used to describe the non-bonding interactions. After a first optimization of the unit cells, the most stable structure has been selected by optimizing individually the 10 most stable frames obtained in a molecular dynamics run (NPT, 200 ps (frames saved every 200 fs), $P = 1$ atm, $T = 340$ K) and by choosing among them the lowest in energy. X-ray diffractograms were simulated for the most stable structures with the Cerius2 package [22] (X-ray source: Copper (wavelength of 1.5418 Å); peaks were simulated with Lorentzian functions (FWHM = 0.06°)). The lattice parameters of the unit cell (length of the crystal axes and angles between them) were ultimately refined so that the relative intensities of the X-ray peaks in the simulation best match the experimental results. During this last step, the values assigned to the cell parameters were kept frozen and only the conformations of the molecules within the unit cell have been fully optimized with the COMPASS force field.

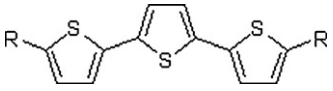

Fig. 1. Chemical structure of dialkylterthiophene: –R is for $-C_nH_{2n+1}$ where $n = 5–10$. The molecular length varies from 25.3 Å for $-C_5H_{11}$ to 38.0 Å for $-C_{10}H_{21}$.

4. Results and discussion

4.1. Thermotropic behaviour

Several liquid crystal phases were observed by DSC and their nature were determined using XRD, POM and the simulation tools. Fig. 2 shows the DSC curves for diheptylterthiophene (Fig. 2a) and dihexylterthiophene (Fig. 2b). We can observe various phase transitions, from crystalline, to the various smectic phases and to the isotropic phase (a first-order character for the Kr/Sm and Sm/Iso phase transitions and a second order character for the Sm/Sm transitions). Table 1 reports a summary of the observations for the different compounds (**1**–**6**): the phase transitions (from crystalline, Cr, to the various smectic phases, SmC, SmF, SmG, and to the isotropic phase, I), the transition temperature *T*, the transition enthalpy ΔH and the isotropic entropy (ΔS_m). The isotropic entropy ΔS_m was calculated from enthalpy values ($\Delta S_m = \Delta H/T$).

From Table 1 we remark that most of the transition temperatures increase with the length of the alkyl chain. For example, the Cr/SmG transition temperature is equal to 52 °C for diheptylterthiophene and to 64 °C for dioctylterthiophene. This observation can be corre-

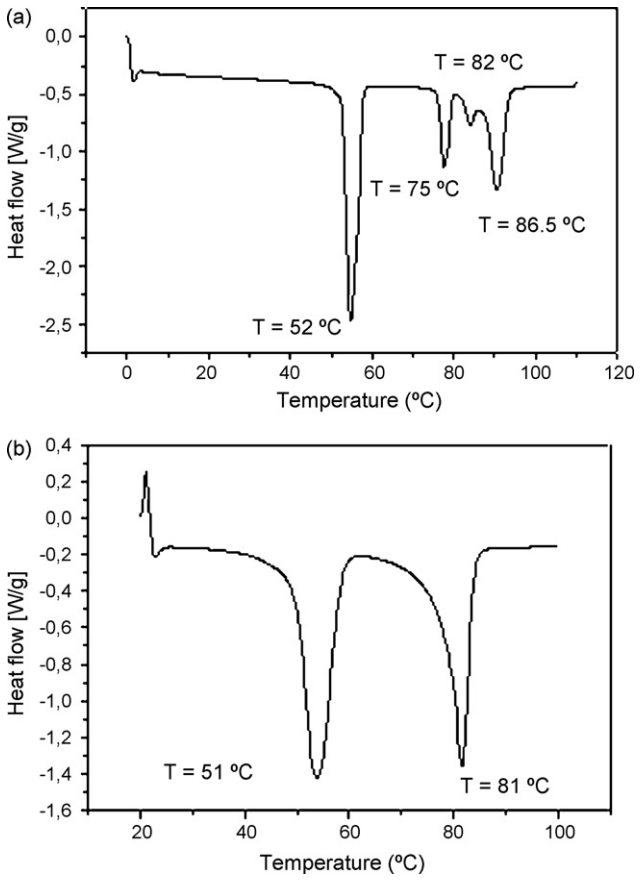

Fig. 2. DSC curves of diheptylterthiophene **3** (a, top) and dihexylterthiophene **2** (b, bottom), shown as an example.

Table 1
Thermotropic behaviour of dialkylterthiophenes studied by differential scanning calorimetry (DSC) at a heating rate of 5 °C min^{-1}. Cr stands for crystalline phase, Sm for smectic phase of various nature (C, F or G), and I for the isotropic phase. The error on the enthalpy is on the order of 0.3 kJ mol^{-1}, and the error on the fusion entropy on the order of 0.2 J K^{-1} mol^{-1}. In parenthesis, isotropic entropic values are calculated from previous published values for comparison [12].

Compound	Transition temperature/°C [enthalpy/kJ mol^{-1}]	ΔS_f (J K^{-1} mol^{-1})
1 (–C_5H_{11})	**Cr** 46 [15.2] **SmG** 76 [13.6] **I**	38.9 ([12] 35.3)
2 (–C_6H_{13})	**Cr** 51 [16.7] **SmG** 81 [16.4] **I**	46.3 ([12] 56.2)
3 (–C_7H_{15})	**Cr** 52 [17.8] **SmG** 75 [3.8] **SmF** 82 [0.7] **SmC** 86 [7] **I**	19.4 ([12] 28.2)
4 (–C_8H_{17})	**Cr** 64 [24.4] **SmG** 71 [3.3] **SmF** 85 [1.6] **SmC** 90 [7.3] **I**	20.1 ([12] 27.5)
5 (–C_9H_{19})	**Cr** 66 [30.8] **SmF** 91 [1.8] **SmC** 94 [10.4] **I**	28.3 ([12] 36.9)
6 (–$C_{10}H_{21}$)	**Cr1** 43 [2.3] **Cr2** 71 [32.1] **SmF** 92 [2.7] **SmC** 95 [10.5] **I**	28.6

lated with the evolution of the transition temperature for alkanes. In the latter case, each additional CH_2 induces an increase of the melting and boiling temperatures [23]. However, in contrast to alkanes, no odd–even effect is observed here [23], since, for each compound, the number of carbon atoms is even due to the symmetrical conformation of the alkyl chain (2*Cn). Therefore, the disposition of the end group tends to enhance the molecular anisotropy [24].

The enthalpy of each type of transition also increases with the number of carbon atoms. Moreover, we remark that the enthalpy values for the Cr/Sm phase transition are much higher (15.2–32.1 kJ mol^{-1}) than for the Sm/Sm transitions (0.7–3.8 kJ mol^{-1}) and the Sm/Iso transitions (7.0–16.4 kJ mol^{-1}). We expected these results which can be correlated with the results found for 4′-octyl-4-biphenylcarbonitrile (8CB). For the latter, the enthalpy value found for the Cr/SmA phase transition was higher (∼25 kJ mol^{-1}) than for the SmA/Nematic and Nematic/Iso transitions (∼1.4 and 0.612 kJ mol^{-1}), respectively [25,26]: the larger the difference between the molecular organisation of the two phases, the larger the transition enthalpy.

As it is the case for alkanes, ΔS_m increases with the number of carbon atoms. There is a second effect, related to the number of phase transitions between the first crystalline phase and the isotropic phase. For alkanes, the isotropic entropy decreases when going from octane (95.9 J K^{-1} mol^{-1}) to nonane (70.4 J K^{-1} mol^{-1}) due to the existence of two crystalline phases in nonane, giving rise to an additional transition compared to octane [23]. This also holds true for dialkylterthiophenes: an increase in the number of phase transitions induces a decrease of ΔS_m. Indeed, we note a higher isotropic entropy value for dihexylterthiophene (ΔS_m = 46.3 J K^{-1} mol^{-1}) compared to diheptylterthiophene (ΔS_m = 19.4 J K^{-1} mol^{-1}), which is consistent with the observation done by Byron et al. in a previous study (Table 1) [12].

Previous studies of the cyanobiphenyl homologous series (5CB–12CB) have shown the influence of the length of the alkyl chains on the molecular organisation and hence on the nature of the liquid crystal phases [27]. Our results point to a similar influence of the aliphatic chains for the compounds studied. For dialkylterthiophenes having short alkyl chains like dihexylterthiophene, the fluidity provided by the presence of alkyl chains is quite restricted so that the only liquid crystal phase observed for this compound is a smectic G phase also called "crystal G". This type of phase is close to a crystalline phase (see XRD and simulation studies). Moreover, for compounds having longer alkyl chains such as dinonylterthiophene, we note the disappearance of phase SmG, and the appearance of more disordered smectic phases such as the SmF and SmC phases.

4.2. Structural analysis

In the series of dialkylterthiophenes synthesised, we can estimate the length of the molecules considering that the size of an alkyl chain is (0.15 + 0.127 × n) nm with n the number of carbon atoms [28], and the size of terthiophene is 12.14 Å [29].

Fig. 3 shows two examples of X-ray diffraction patterns: for didecylterthiophene **6** in the SmC phase and for dihexylterthiophene **2** in the SmG phase.

In general, we observe a series of three to four intense reflections in the low region part of the spectrum (see Fig. 3): the first Bragg reflection (1 0 0) corresponding to the smectic layer thickness and higher order reflection peaks. By comparing the thickness of the smectic layer obtained from the X-ray measurements with the calculated length of molecule, we deduce by considering the molecule as a rigid rod that the long axis of the molecules is tilted in each smectic phase ("apparent" tilt angle). A variation of the "apparent" tilt angle is observed between the SmC, SmF and SmG phases. The tilt is more pronounced for the SmG phase (∼27–31°) than for the SmF or SmC (∼16–18°). In order to explain this phenomenon, it is desirable to have some information on the molecular packing in each smectic phase. For the SmG phase, we observe some peaks at high q-values (Fig. 3 bottom) corresponding to an in-plane structure. The Bragg reflections represent interplanar distances that can be related to a 3D molecular organization. This structure (con-

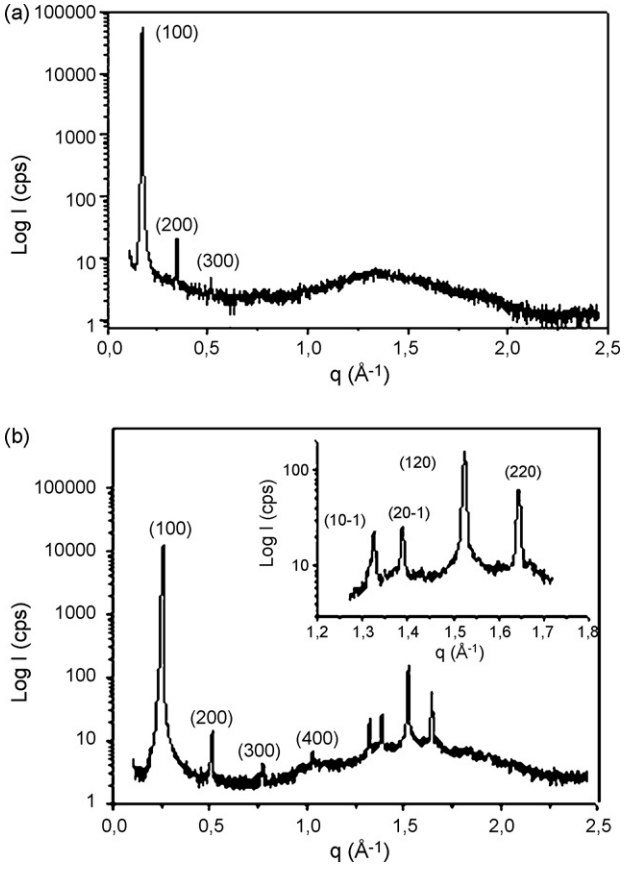

Fig. 3. X-ray diffraction patterns: (a) for didecylterthiophene **6** in the SmC phase, and (b) for dihexylterthiophene **2** in the SmG phase (see text for details).

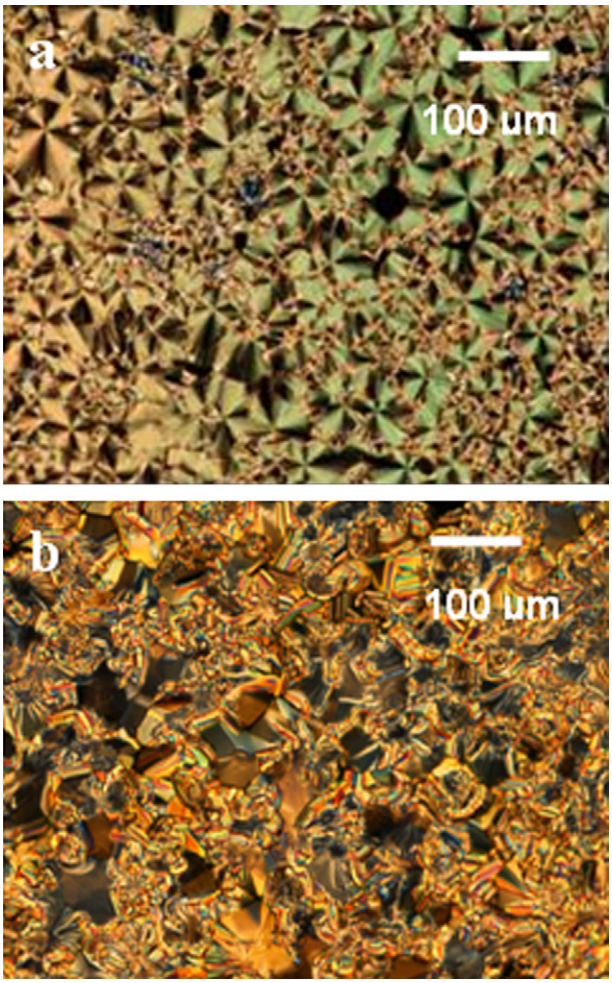

Fig. 4. POM images of the liquid crystal compounds: (a, top) for the SmC phase (T = 87 °C) of dinonylterthiophene **5** and (b, bottom) for the SmG phase (T = 67 °C) of dihexylterthiophene **2**.

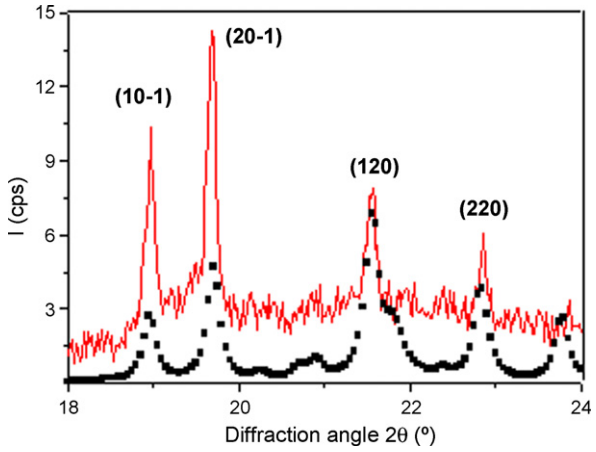

Fig. 5. Simulated X-ray diffractograms (black dots) superposed to the experimental X-ray diffractograms (line) for compound **4**.

firmed by the simulations) is characteristic of Π–Π stacking in two directions with strong intermolecular contacts between neighbouring sulphur atoms, and a high alkyl chain density inducing a large "apparent" tilt angle [17,30]. The inter-planar distances (from 3.8 to 4.74 Å) for dihexylterthiophene **2** confirm the distances (from 4.16 to 4.63 Å) measured previously for dioctylterthiophene by Funahashi and Hanna [31,32]. As described previously, in the SmF and SmC phases, the molecules have a higher degree of freedom due to low or the absence of molecular organization (we only observe a halo related to the alkyl chains at around q = 1.4 Å^{-1}) within the smectic layers [33]. The SmC phase has a more fluidic texture than the SmG phase [34]. This assumption is confirmed by POM in Fig. 4 showing a typical focal conic texture characteristic of a SmC phase and a mosaic texture characteristic of highly ordered SmG smectic phase [34,35]. Moreover, topologic defects such as free dislocations may also appear, as suggested by other authors [33,36]. Therefore, the higher mobility of the molecules can explain a reduced tilt angle.

The XRD data are consistent with the disordered nature of the smectic phases such as smectic C and F phases but they do not allow us to affirm that the nature of the ordered smectic phase is SmG. However, using simulation tools, one is able to determine the molecular packing of the compound in this liquid crystal phase, to define the corresponding lattice parameters and to calculate the density.

Fig. 5 shows the simulated and experimental X-ray diffractograms for dioctylterthiophene **4** (in a limited range of diffraction angles for the sake of clarity). Table 2 summarises the peak indices and the relative inter planar distance determined from the simulations for compounds **1**–**4**. The relative intensity of the intra-layer peaks compared to the inter-layer peaks is overestimated since the disorder within the smectic layer is systematically underestimated in our simulations because of the periodic boundary conditions. The unit cells reproducing the experimental X-ray diffractograms of the four substituted terthiophenes are displayed in Fig. 6 and reveal a tilted molecular packing for each system, characteristic of a SmG phase ("Crystal G"). Within the unit cells, the two molecules adopt an anti-parallel arrangement so that their dipole moments cancel each other. The parameters of the unit cells are similar for the four compounds: see Table 3 and also Fig. 6, except for the crystal axis

Table 2
Simulated reflections and interplanar spacing in compounds **1**–**4**.

Compound **1** (C5TTC5)		Compound **2** (C6TTC6)		Compound **3** (C7TTC7)		Compound **4** (C8TTC8)	
Index	d (Å)	Index	d (Å)	Index	d (Å)	Index	d (Å)
(1 0 0)	21.22	(1 0 0)	24.16	(1 0 0)	26.40	(1 0 0)	29.05
(0 1 0)	8.58	(0 1 0)	8.65	(0 1 0)	8.53	(0 1 0)	8.58
(1 1 0)	7.44	(3 0 0)	8.05	(1 1 0)	7.70	($\bar{2}$ 1 0)	8.16
(2 1 0)	6.09	(1 1 0)	7.65	(2 1 0)	6.61	(1 1 0)	7.80
(4 0 0)	5.31	(3 $\bar{1}$ 0)	6.62	(4 0 0)	6.60	(4 0 0)	7.26
(0 0 1)	4.84	(2 1 0)	6.43	(0 0 1)	4.77	(2 1 0)	6.79
(1 0 $\bar{1}$)	4.73	(4 0 0)	6.04	(1 0 $\bar{1}$)	4.71	(1 0 $\bar{1}$)	4.68
(2 0 $\bar{1}$)	4.42	(0 0 1)	4.81	(2 0 $\bar{1}$)	4.50	(2 0 $\bar{1}$)	4.51
(0 2 0)	4.29	(1 0 $\bar{1}$)	4.73	(0 2 0)	4.26	(1 2 0)	4.12
(0 1 $\bar{1}$)	4.13	(2 0 $\bar{1}$)	4.48	(1 2 0)	4.09	(2 2 0)	3.90
(1 2 0)	4.05	(1 2 0)	4.11	(2 1 $\bar{1}$)	4.01	(3 $\bar{1}$ $\bar{1}$)	3.74
(2 2 0)	3.72	(2 2 0)	3.83	(3 1 $\bar{1}$)	3.85	(3 2 0)	3.65

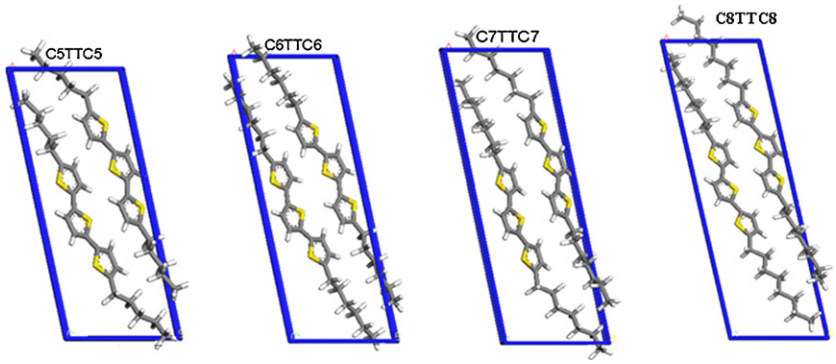

Fig. 6. Representation of the unit cells for the four terthiophene derivatives.

linked to the length of the molecule which increases with the size of the alkyl chain. The unit cells are all triclinic.

The densities calculated for compounds **1**–**4** (1.37, 1.29, 1.30 and 1.25 g cm^{-3}, respectively) are in accordance with the density values found in the literature for dihexylquaterthiophene (1.23 and 1.33 g cm^{-3} in crystalline phase) [37,38].

The cofacial distances d_c (see Fig. 7) between the aromatic cores are quite similar whatever the length of the alkyl chains (from 3.2 to 3.0 Å for the compounds studied). However, the decrease in the alkyl chain length is accompanied by a small reduction in the intermolecular distance since the equilibrium distance between two alkyl chains is larger than that between two conjugated cores. The S–S distances lie between 3.92 and 5.20 Å, in agreement with the S–S distances reported (3.69–4.95 Å) in the literature [1,11,39].

In all cases, the two molecules in the unit cell are translated with respect to one another, by a different distance (d_{tr}) (Fig. 6): 2.1, 3.0, 4.0 and 3.1 Å for compounds **2**, **1**, **3** and **4**, respectively. The amplitude of the translation is correlated to the tilt angle (τ) of the aromatic core within the cell; the larger the tilt angle of the aromatic core (29°, 24°, 17° and 20° for compounds **2**, **1**, **3** and **4**, respectively), the smaller the amplitude of the translation. By comparison with the "apparent" tilt angle calculated for the whole structure (29°, 31°, 26° and 27° for compounds **2**, **1**, **3** and **4**, respectively), the values of (τ) reveal a strong influence of the length of the alkyl chains on the torsion angles between the terthiophene core and the alkyl chains, going from 15° for compound **1** to 39° for compound **4**.

Finally, the correlation length in the direction normal to the layer was estimated for each compound (Fig. 8) by fitting the (1 0 0) reflection with a Lorentzian curve, using the Scherer's formula and taking into account the instrumental resolution of 0.02°. We estimate for the SmF or SmC phase a correlation length of about 1900 Å (~59 layers) while for the SmG phase (which is a more ordered smectic phase) the correlation length is around 1400 Å (~50 layers). This might be rationalized by the fact that the SmG phase presents defects such as stacking faults or subboundaries between the smectic planes [40]. These defects are due to dislocations from SmC and SmF phases, which are trapped by the growth front into the smectic

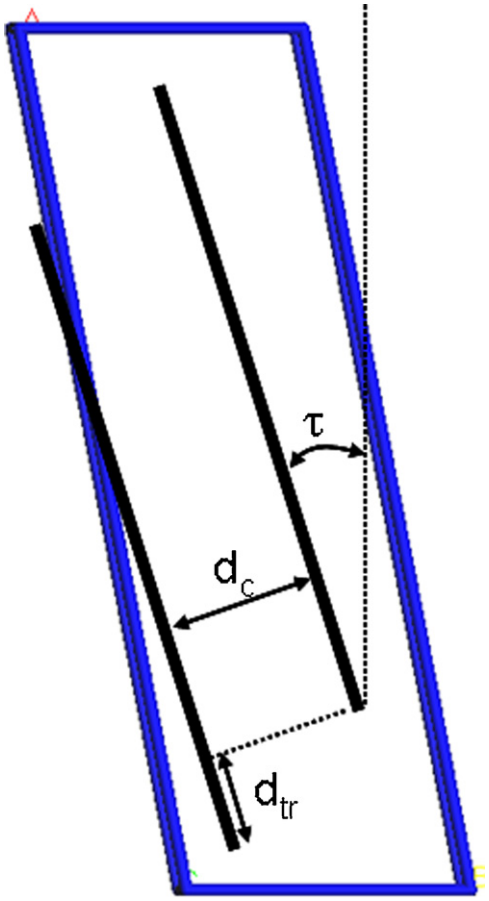

Fig. 7. Illustration of the various geometric parameters used in the conformational analysis.

Table 3
Structural data for compounds **1**–**4**.

Lattice parameters	Compound **1** (C5TTC5)	Compound **2** (C6TTC6)	Compound **3** (C7TTC7)	Compound **4** (C8TTC8)
a (Å)	21.7	24.7	26.9	29.5
b (Å)	8.79	8.85	8.70	8.78
c (Å)	4.85	4.82	4.78	4.75
α (°)	87	87	93	93
β (°)	91	91	90	89.3
γ (°)	102	102	101	102
V (Å^3)	925.1	1053.6	1118.7	1230.3
Calculated density (g cm^{-3})	1.37	1.29	1.30	1.25

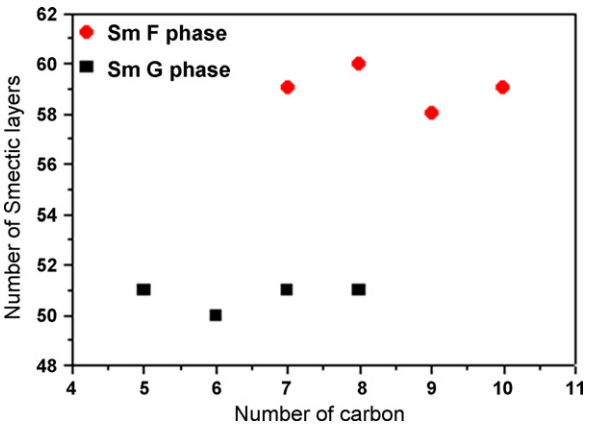

Fig. 8. Correlation length of the reflection (1 0 0) in the smectic G and F phases as a function of the length of the alkyl chains.

G phase and become imperfect dislocations to which the stacking faults are coupled [41].

5. Conclusion

We have presented a detailed study of the liquid crystal phases of dialkylterthiophenes. The X-ray diffraction study support the DSC results and shows that the liquid crystal phases are smectic C, F, and G phases. The X-ray diffraction study also indicates that the structural properties depend on the nature of the smectic phases and the length of the alkyl chains. For compounds **1**–**4** ($-C_5H_{11}$, $-C_6H_{12}$, $-C_7H_{15}$, $-C_8H_{17}$), the XRD analyses have revealed a molecular organisation within the smectic layers connected to a SmG phase. The corresponding structures have been described by molecular mechanics simulations pointing in each case to a triclinic cell. Oligothiophene thin films deposited on silicon or glass substrate could also be explored in the future to determine the molecular ordering at the film/substrate interface. Indeed in Pentacene thin film, Cheng et al. identify a different morphology of the crystalline phase at the interface substrate/film [42]. Such behaviour of molecular organisation of dialkylterthiophenes could have important effects on the charge carrier mobility of OFETs.

Acknowledgments

We acknowledge financial support by the Région Wallonne via the project ETIQUEL. Research in Mons is also supported by the Science Policy Office of the Belgian Federal Government (PAI 6/27) and FNRS-FRFC. JC is an FNRS research fellow.

References

[1] D. Fichou, J. Mater. Chem. 10 (2000) 571.
[2] D. Fichou, Handbook of Oligo- and Polythiophenes, Wiley-VCH, New York, 1999.
[3] M. Funahashi, J. Hanna, Chem. Phys. Lett. 397 (2004) 319.
[4] V. de Cupere, J. Tant, P. Viville, R. Lazzaroni, W. Osikowicz, W.R. Salaneck, Y.H. Geerts, Langmuir 22 (2006) 7798.
[5] F. Dinelli, M. Murgia, P. Levy, M. Cavallini, F. Biscarini, D.M. de Leeuw, Phys. Rev. Lett. 92 (2004) 116802.
[6] H. Sirringhaus, P.J. Brown, R.H. Friend, M.M. Nielsen, K. Bechgaard, B.M.W. Langeveld-Voss, A.J.H. Spiering, R.A.J. Janssen, E.W. Meijer, P. Herwig, D.M. de Leeuw, Nature 401 (1999) 685.
[7] J. Zak, M. Lapkowski, S. Guillerez, G. Bidan, Synth. Met. 152 (2005) 185.
[8] F. Geiger, G. Marowsky, Chem. Phys. Lett. 254 (1996) 179.
[9] X. Tang, X. Baie, J.-P. Colinge, A. Crahay, B. Katschmarskyj, V. Scheuren, D. Spôte, N. Reckinger, F. Van de Wiele, V. Bayot, Solid-State Electron. 44 (2000) 2259.
[10] C. Van Haesendonck, L. Stockman, R.J.M. Vullers, Y. Bruynseraede, L. Langer, V. Bayot, E. Grivei, J.-P. Issi, J.-P. Heremans, C.H. Olk, Surf. Sci. 386 (1997) 279.
[11] G. Horowitz, Adv. Mater. 10 (1998) 365.
[12] D. Byron, A. Mataharu, R. Wilson, G. Wright, Mol. Cryst. Liq. Cryst. 165 (1995) 61.
[13] M. Funahashi, J.-I. Hanna, Mol. Cryst. Liq. Cryst. 368 (2001) 4078.
[14] M. Funahashi, J. Hanna, Appl. Phys. Lett. 76 (2000) 2574.
[15] I.P.M. Bouchoms, W.A. Schoonveld, J. Vrijmoeth, T.M. Klapwijk, Synth. Met. 104 (1999) 175.
[16] J. Leroy, J. Levin, S. Sergeyev, Y. Geerts, Chem. Lett. 35 (2006) 166.
[17] J. Leroy, N. Boucher, S. Sergeyev, M. Sferrazza, Y.H. Geerts, Eur. J. Org. Chem. 128 (2007) 1256.
[18] P.J. Collins, M. Hird, Introduction to Liquid Crystals: Chemistry and Physics, Taylor & Francis, 2004.
[19] H. Sun, J. Phys. Chem. B 102 (1998) 7338.
[20] MS Modeling v4.0.0.0, Accelrys Software Inc., 2005.
[21] P.P. Ewald, Ann. Phys. 64 (1921) 253.
[22] Cerius2; Accelrys: San Diego, 1997.
[23] J. Israelachvili, Intermolecular and Surface Forces, 2d ed., Elsevier Science and Technology Books, 1992.
[24] S. Chandrasekhar, Liquid Crystals, 2nd ed., 2004.
[25] J. Thoen, H. Marynissen, W. Van Dael, Phys. Rev. A 26 (1982) 2886.
[26] G.W. Smith, Mol. Cryst. Liq. Cryst. 41 (1977) 89.
[27] S.J. Woltman, G.D. Jay, G.P. Crawford, Nat. Mater. 6 (2007) 929.
[28] C. Tanford, The Hydrophobic Effect: Formation of Micelles and Biological Membranes, New York, Wiley, 1980.
[29] B. Gombojav, N. Namsrai, T. Yoshinari, Shin-Ichiro, Nagasaka, H. Itoh, K. Koyama, J. Solid State Chem. 177 (2004) 2827.
[30] K.R. Amundson, H.E. Katz, A.J. Lovinger, Thin Solid Films 426 (2003) 140.
[31] M. Funahashi, J.-I. Hanna, Adv. Mater. 17 (2005) 594.
[32] M. Funahashi, J.-I. Hanna, Chem. Phys. Lett. 397 (2004) 319.
[33] P. Oswald, P. Pieranski, Les cristaux liquides, TOME 1 and 2: Gordon and Breach Science Publishers, 2000 and 2002.
[34] I. Dierking, Texture of Liquid Crystals, Wiley-VCH, 2003.
[35] G.W. Gray, J.W.G. Goodby, Smectic Liquid Crystals, Leonard Hill, Philadelphia, 1984.
[36] E. Smela, L.J. Martinez-Miranda, J. Appl. Phys. 73 (1993) 3299.
[37] F. Garnier, R. Hajlaoui, A. El Kassmi, G. Horowitz, L. Laigre, W. Porzio, M. Armanini, F. Provasoli, Chem. Mater. 10 (1998) 3334.
[38] M. Moret, M. Campione, A. Borghesi, L. Miozzo, A. Sassella, S. Trabattoni, B. Lotz, A. Thierry, J. Mater. Chem. 15 (2005) 2444.
[39] F. Van Bolhuis, H. Wynberg, E.E. Havinga, E.W. Meijer, E.G.J. Staring, Synth. Met. 30 (1989) 381.
[40] T. Börzsönyi, S. Akamatsu, G. Faivre, Phys. Rev. E 65 (2001) 011702.
[41] P. Oswald, L. Lejcek, J. Phys. II. France 9 (1991) 1067.
[42] H.L. Cheng, Y.-S. Mai, W.-Y. Chou, L.-R. Chang, X.-W. Liang, Adv. Funct. Mater. 17 (2007) 3639.